Research article

Danlou tablet alleviates sepsis-induced acute lung and kidney injury by inhibiting the PARP1/HMGB1 pathway

Yongjing Yu [a,b,c], Zhixi Li [a,b,c], Chang Liu [a,b,c], Yue Bu [a,b,d], Weidong Gong [a,b],
Juan Luo [a,b], Ziyong Yue [a,b,*]

[a] *Department of Anesthesiology, Second Affiliated Hospital of Harbin Medical University, 246 Xuefu Road, Harbin, 150001, China*
[b] *The Key Laboratory of Anesthesiology and Intensive Care Research of Heilongjiang Province, 246 Xuefu Road, Harbin, 150001, China*
[c] *The Key Laboratory of Myocardial Ischemia Organization, Chinese Ministry of Education, 246 Xuefu Road, Harbin, 150001, China*
[d] *Department of Pain Medicine, Second Affiliated Hospital of Harbin Medical University, 246 Xuefu Road, Harbin, 150001, China*

A R T I C L E   I N F O

A B S T R A C T

Background: Sepsis-associated acute lung injury (ALI) and acute kidney injury (AKI) are common complications that significantly impact patient prognosis. Danlou tablet (DLT) is a traditional herbal preparation with anti-inflammatory and antioxidant properties. However, its therapeutic potential in sepsis remains unknown.
Methods: The impact of DLT on ALI and AKI was evaluated using the cecal ligation and puncture (CLP) experimental sepsis animal model. The effects of DLT on macrophages were observed through LPS-stimulated RAW264.7 cell line. Inflammatory cytokines, oxidative stress indicators, HE, PAS, and DHE staining, lung wet-to-dry weight ratio, and serum creatinine and urea nitrogen levels were used to assess tissue injury. Network pharmacology, molecular docking, and molecular dynamics simulations were used to explore the potential regulatory mechanisms of DLT in sepsis. Western blot and immunohistochemical staining were used to validate the expression of mechanism-related proteins.
Results: DLT inhibited the inflammatory response and oxidative stress, improved structural and functional abnormalities in lung and kidney tissues in CLP mice, and alleviated pro-inflammatory responses of LPS-stimulated macrophages. PARP1 and HMGB1 were identified as key regulatory targets. The results of in vitro and in vivo experiments suggest that DLT can effectively inhibit PARP1/HMGB1 and improve sepsis-associated ALI and AKI.
Conclusion: The present study demonstrated that DLT suppressed pro-inflammatory responses of macrophage and alleviated ALI and AKI in the CLP mice by inhibiting the transition activation of PARP1/HMGB1. These findings partially elucidate the mechanism of DLT in sepsis-associated ALI and AKI and further clarify the active components of DLT, thereby providing a scientific theoretical basis for treating sepsis with DLT.

1. Introduction

Sepsis is a dysregulated inflammatory response caused by infection [1], posing a severe threat to health as a principal cause of

---

* Corresponding author. Department of Anesthesiology, Second Affiliated Hospital of Harbin Medical University, 246 Xuefu Road, Harbin, 150001, China.
E-mail address: yueziyong@hrbmu.edu.cn (Z. Yue).

infection-related deaths globally [2]. Organ dysfunction due to sepsis is the primary cause of death in septic patients [3]. Notably, acute lung injury (ALI) and acute kidney injury (AKI) induced by sepsis are common complications, both of which occur early in sepsis and increase the mortality rate of septic patients [4,5]. Moreover, studies have found that ALI and AKI caused by sepsis can act as initiators and modulators of each other, thereby exacerbating the patient's inflammatory response, which is detrimental to prognosis [6–8]. Therefore, effectively alleviating ALI and AKI induced by sepsis has positive significance for improving the prognosis of sepsis. Immune cells, including macrophages, mediate excessive inflammatory reactions and oxidative stress, representing crucial factors in the development of organ dysfunction in sepsis [9]. Consequently, the effective control of exaggerated inflammatory responses and oxidative stress holds significance for the therapeutic intervention of sepsis-induced organ dysfunction.

Currently, clinical practice sepsis treatment primarily involves fluid resuscitation, infection treatment, anticoagulation treatment, and glucocorticoids. Nevertheless, treatment outcomes remain far from ideal, and there needs to be more specific, reliable therapeutic approaches [1]. Traditional Chinese medicine (TCM) is gaining recognition for its safety and effectiveness. It is believed that TCM has unique advantages in treating inflammatory diseases such as sepsis [10]. Modern TCM generally classifies sepsis as a "hot disease". Based mainly on the theories of the "Treatise on Cold Damage Diseases" and the doctrine of warm diseases, TCM primarily explains the pathogenesis of sepsis as "toxic stasis deficiency". It mainly uses heat-clearing, detoxifying, blood-activating, and stasis-removing drugs to assist positive qi in the later stages, often achieving satisfactory clinical effects [11]. Therefore, it is beneficial to extensively explore TCM formulas capable of treating sepsis and to clarify further the practical components and mechanisms of action of these drugs for treating sepsis. Danlou tablet (DLT) is a traditional herbal preparation whose main components are *Trichosanthes kirilowii* Maxim, *Salvia miltiorrhiza* Bunge, *Ligusticum chuanxiong* S.H.Qiu, Y.Q.Zeng, K.Y.Pan, Y.C.Tang & J.M.Xu, *Allium macrostemon* Bunge, *Paeonia lactiflora* Pall, *Pueraria lobata* (Willd.) Ohwi, *Alisma plantago-aquatica* L., *Astragalus membranaceus* (Fisch.) Bunge, *Davallia mariesii* T. Moore ex Baker, *Curcuma aeruginosa* Roxb. DLT has been shown to have a favorable inhibitory effect on the inflammatory response and oxidative stress, thereby exerting organ-protective effects [12–14]. Additionally, DLT has been demonstrated to effectively alleviate cellular apoptosis [15]. Despite the confirmed therapeutic efficacy of DLT, whether it can mitigate organ dysfunction induced by sepsis and its specific mechanisms remain unknown, warranting further clarification.

In this study, we initially established a septic mouse model using the cecal ligation and puncture (CLP) method to evaluate the therapeutic efficacy of DLT. Our results demonstrate that DLT effectively alleviates systemic inflammatory responses and oxidative stress in CLP mice, mitigating structural and functional damage in lung and kidney tissues. Furthermore, we employed network pharmacology to explore the underlying mechanisms and identify active compounds in DLT in treating sepsis. Through bioinformatics analysis combined with molecular docking techniques, we identified PARP1 and its downstream target, HMGB1, as crucial regulatory targets in this process. In vivo and in vitro experiments indicate that DLT attenuates macrophage-driven pro-inflammatory responses and oxidative stress by inhibiting the PARP1/HMGB1 signaling pathway, thereby alleviating sepsis-induced ALI and AKI. In summary, this study elucidates the therapeutic role of DLT in sepsis and unveils the underlying mechanisms, providing a new theoretical foundation for DLT in treating sepsis.

2. Materials and methods

2.1. Experimental animals, chemicals, and reagents

The experimental animals were purchased from the Animal Experiment Center of the Second Affiliated Hospital of Harbin Medical University and kept in a constant temperature and humidity environment. All mice had a 12-h light-dark cycle and had free access to food and water. Animal experiments were conducted in strict accordance with the National Institutes of Health guidelines and approved by the Ethics Committee of the Second Affiliated Hospital of Harbin Medical University (Approval No. SYDW 2021-087, Harbin, China).

The DLT (batch number: 20140302) was purchased from Jilin Connell Pharmaceutical Co. Ltd., China. LPS (O111: B4, L2630) was purchased from Sigma-Aldrich (St. Louis, MO, USA). Olaparib (HY-10162) was obtained from MedChemExpress (NJ, USA). GSSG, MDA, DHE, DAPI, and Hoechst 33342 were purchased from Beyotime Biotechnology (Shanghai, China). ELISA kits for mouse TNF-α, IL-6, and IL-1β and microplate assay kits for creatinine and blood urea nitrogen were provided by Jianglai Co., Ltd. (Shanghai, China). HE and PAS staining kit were purchased from Solarbio (Beijing, China). Primary antibody sources are as follows: PARP1 (DF7198; Affinity, OH, USA), HMGB1 (ab79823; Abcam, Cambridge, UK), and β-actin (AC026; ABclonal, Wuhan, China).

2.2. Procedure of cecum ligation and puncture

This experiment utilized 6-8-week-old C57BL/6 mice to establish a sepsis animal model. Following previous literature [16], the cecum ligation and puncture (CLP) method was employed to simulate sepsis. Briefly, mice were induced with 3 % isoflurane for anesthesia, maintained at 1.5 % concentration. A midline abdominal incision was made, and layers of tissues were sequentially dissected to locate the cecum. The cecum was ligated at the distal one-half, followed by a puncture at the blind end. After the procedure, the incision was sutured layer by layer, and mice were subjected to fluid resuscitation before being returned to their cages for recovery. Throughout the procedure, attention was given to maintaining adequate warmth for the mice.

2.3. Durg administration and animal grouping

The DLT was diluted with normal saline for animal experiments. The dosage and method of animal administration were referred to

previous literature [14,17]. Mice in the treated groups received daily intragastric administration of the drug for seven consecutive days before modeling, with cecal ligation and puncture (CLP) performed 2 h after the final administration. The experimental groups were as follows: 1) Sham group: Mice received daily intragastric saline for seven days and underwent surgical procedures excluding ligation and puncture on the seventh day. 2) CLP group: Mice received daily intragastric saline for seven days and underwent CLP on the seventh day. 3) DL-L group: Mice received intragastric administration of a low dose (1400 mg/kg/day) of DLT for seven days and underwent CLP on the seventh day. 4) DL-H group: Mice received intragastric administration of a high dose (2800 mg/kg/day) of DLT for seven days and underwent CLP on the seventh day. After 24 h of CLP, blood was collected via cardiac puncture under deep iso-flurane anesthesia. Subsequently, tissues from euthanized mice were collected and processed.

2.4. Preparation of drug-containing serum

Based on previous literature [18], 6-8-week-old C57BL/6 mice were divided into the following groups: blank serum group, low-dose DLT group (1400 mg/kg/day), and high-dose DLT group (2800 mg/kg/day). Intragastric administration of normal saline or different doses of DLT was carried out continuously for seven days. The serum was collected 1 h after the final administration. The collected serum was centrifuged at 3,000 rpm for 10 min and filtered through a 0.22 μm filter. The drug-containing serum was heat-inactivated at 56 °C and stored at −80 °C for future use.

2.5. Cell culture and treatment

RAW264.7 cells were cultured in high-glucose DMEM supplemented with 10 % FBS and 1 % penicillin-streptomycin. Cells in the logarithmic growth phase were used for experiments. To simulate changes in macrophages under septic conditions, cells were treated with LPS at a final concentration of 1 μg/ml for 24 h. RAW264.7 cells were categorized into the following groups based on different treatments:1) Control group: Cultured with 10 % serum from mice in the blank group. 2) LPS group: Cultured with 10 % serum from mice in the blank group + LPS. 3) DL-L group: Cultured with 10 % serum from mice in the low-dose DLT group + LPS. 4) DL-H group: Cultured with 10 % serum from mice in the high-dose DLT group + LPS.

2.6. Prediction of the active ingredients and targets of DLT

The Traditional Chinese Medicines Systems Pharmacology Platform (TCMSP, http://tcmspw. com/tcmsp.php) was used to predict the active ingredients and effective targets in DLT components. The criteria for screening active ingredients were oral bioavailability (OB) ≥ 30 % and drug-likeness (DL) ≥ 0.18. Subsequently, the corresponding targets of the screened active ingredients were obtained, and gene symbols were annotated using the gene map from the UniProt database to obtain DLT-related targets.

2.7. Identification of sepsis-related targets

Sepsis-related datasets, including GSE26440, GSE28750, GSE57065, GSE65682, and GSE95233, were retrieved from the Gene Expression Omnibus (GEO) database (https://www.ncbi.nlm.nih.gov/geo/). Differential analysis of these datasets was performed using R language to identify sepsis-related differentially expressed genes, with p.adj <0.05 and |logFC| > 1 as the threshold. Taking SEPSIS as keyword, the sepsis related genes with scores ≥1 were obtained from GeneCards (https://www.genec ards.org/). Simul-taneously, genes related to sepsis were retrieved fromOnline Mendelian Inheritance in Man (OMIM, https://omim.org/), DrugBank (https://www.drugbank.com/), and the Therapeutic Target Database (TTD, https://db.idrblab.net/ttd/) with SEPSIS as the keyword. The combination of sepsis-related differentially expressed genes and sepsis-associated genes from GeneCards, OMIM, DrugBank, and TTD yielded a set of sepsis-related targets.

2.8. Protein–protein interaction and enrichment analysis

The STRING database was employed to construct a protein-protein interaction network for identifying key targets in the treatment of sepsis with DLT. Subsequently, protein clustering analysis was performed using the MCODE plugin with specific parameter settings: Degree Cutoff = 2, Node Score Cutoff = 0.2, K-Core = 2, and Max. Depth = 100.

2.9. Molecular docking

The 3D structures of the receptor proteins PARP1 and HMGB1 were obtained from the Protein Data Bank (PDB, https://www1.rcsb. org/). Using PyMOL 2.3.0 software, water molecules, irrelevant protein chains, and existing ligands were removed. The structures of small-molecule compounds were downloaded from the PubChem database and subjected to force field optimization using Chem3D to achieve the lowest energy conformations. Prior to docking, hydrogenation was applied to the proteins and small molecules using AutoDock. The Grid module was employed to set molecular docking parameters, and a semi-flexible protein-small molecule docking approach from AutoDock Vina was utilized. Ultimately, docking free energy data and docking result files were obtained.

2.10. Molecular dynamics simulation analysis

Molecular dynamics simulations were conducted using Gromacs2019.6 software. Small molecule preprocessing involved the application of AmberTools22 to incorporate the GAFF force field and hydrogenate the molecules using Gaussian 16W for RESP potential calculation. The potential data that was obtained was integrated into the topology file of the molecular dynamics system. Simulations were performed under static conditions at 300K and atmospheric pressure (1 Bar), utilizing the Amber99sb-ildn force field, Tip3p water model for solvent (water molecules), and NaCl counter ions for neutralizing the total charge of the simulation system. The steepest descent method was employed for energy minimization, followed by 100000 steps of isothermal isovolumic ensemble (NVT) equilibrium and isothermal isobaric ensemble (NPT) equilibrium, each with a coupling constant of 0.1 ps and a duration of 100 ps. Subsequently, a free molecular dynamics simulation was executed, consisting of 5000000 steps with a step length of 2 fs, lasting 100 ns. Post-simulation, the built-in tool of the software, was used for trajectory analysis, including the calculation of root-mean-square deviation (RMSD) and root-mean-square fluctuation (RMSF).

2.11. Enzyme linked immunosorbent assay (ELISA)

Blood samples were taken through cardiac puncture 24 h after CLP. After the samples were left to rest overnight at 4 °C, the serum was collected by centrifugation at 3,000 rpm for 15min and stored at −80 °C for later use. In order to obtain cell lysates, the cells were rinsed with pre-cooled PBS, the extraction buffer was added, the cells were scraped and transferred to the centrifuge tube, and incubated on ice for 30 min. Centrifuge at a speed of 13,000 rpm at 4 °C for 10 min and reserve the supernatant at −80 °C for use. According to the manufacturer's instructions, ELISA kits were used to assess the levels of TNF-α, IL-1β and IL-6 in mouse serum and cell lysates, and absorbance were measured at 450 nm.

2.12. Detection of BUN and creatinine

Kidney injury was assessed by measuring serum levels of blood urea nitrogen (BUN) and creatinine. The levels of BUN and creatinine in serum were measured by microplate kit according to the manufacturer's instructions.

2.13. GSSG and GSH content detection

GSSG detection kit was used to determine the content of GSH and GSSG in mouse serum according to the manufacturer's instructions, and absorbance were measured at 412 nm wavelength.

2.14. MDA content detection

MDA detection kit was used to evaluate the lipid peroxidation level in mouse serum according to the manufacturer's instructions and absorbance were measured at 532 nm wavelength.

2.15. HE staining

The mouse lung and kidney tissues were fixed with 4 % formaldehyde and cut into 5 μm sections after conventional embedding with paraffin. After dewaxing in xylene, the slices were rehydrated with gradient ethanol and soaked in distilled water. Then the slices were immersed in hematoxylin dye solution for 10min and washed with distilled water to remove the floating color. After rapid differentiation in the differentiation solution, soak in tap water twice. Apply eosin dye to cover the tissue, pour away excess dye, quickly dehydrate, transparent, and seal the film. The tissue morphology was observed under a microscope and photographed (Olympus Corporation, Tokyo, Japan). Lung and kidney tissue injury score by HE staining were referred to previous literature [19,20].

2.16. PAS staining

The mouse kidneys were fixed with 4 % paraformaldehyde and cut into 5 μm slices after embedding with paraffin. After conventional dewaxing to water, soak in PAS oxidizer for 8min and rinse with distilled water for 3 times. The tissue sections were placed in Schiff staining solution, incubated at room temperature and away from light for 15min, and rinsed with running water. Nuclear staining was performed with hematoxylin staining solution, followed by rapid differentiation by acid differentiation solution, and then rinsed with tap water to reverse blue. After dehydration by ethanol, xylene was applied to make the tissue transparent. The tissue sections were sealed with neutral gum and the morphology was observed under microscope (Olympus Corporation, Tokyo, Japan).

2.17. Lung wet-to-dry weight ratio

The lung wet-to-dry (WD) weight ratio was utilized to assess tissue edema. After euthanasia, mouse lung tissues were weighed to obtain the wet weight. Subsequently, the tissues were dried in an oven at 65 °C for 48 h, and the dry weight was measured. The formula for calculating the wet-to-dry weight ratio is as follows: Wet weight/Dry weight $\times$ 100 %.

2.18. DHE staining

DHE staining was employed to assess the levels of reactive oxygen species in lung and kidney tissues of mice and RAW264.7 cells. The DHE staining solution was prepared to a final concentration of 5 μM for incubating cells or frozen tissue sections. After washing away the excess staining solution, samples were co-stained with Hoechst or DAPI. Finally, the stained tissues or cells were observed and photographed under a fluorescence microscope (DMI4000B; Leica, Wetzlar, Germany). The average fluorescence intensity was calculated using ImageJ software.

2.19. PI staining

PI staining was employed to observe cell death. RAW264.7 cells were plated, and to each milliliter of buffer, 5 μL Hoechst staining solution and 5 μL PI staining solution were sequentially added. After thorough mixing, the cells were incubated at 4 °C for 30 min, washed with PBS, and observed under a fluorescence microscope (DMI4000B; Leica, Wetzlar, Germany). Photographs were taken, and the average fluorescence intensity was calculated using ImageJ software.

2.20. Immunohistochemistry (IHC)

Paraffin sections of lung and kidney tissues were routinely deparaffinized to water. Antigen retrieval was performed in sodium citrate buffer, followed by cooling to room temperature and PBS rinsing. Subsequently, permeabilization was carried out with 0.3 % Triton X-100 for 10 min, followed by washing and blocking with 10 % goat serum for nonspecific antigen site closure. The tissue sections were incubated with the primary antibody at 4 °C overnight, washed with PBS the next day, and then incubated with the
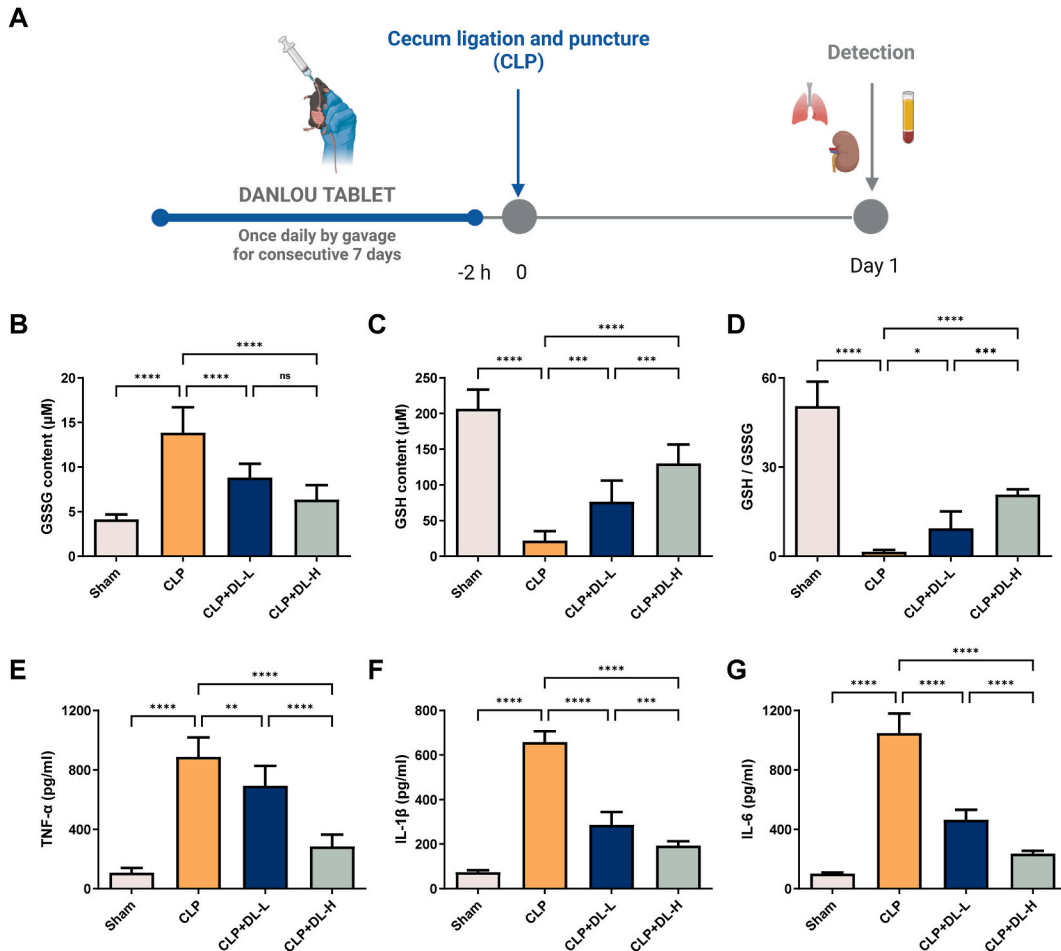
Fig. 1. Danlou tablet attenuates sepsis-induced inflammatory response and oxidative stress. **(A)** The procedure and timeline of in vivo experiments. **(B)** Levels of GSSG in serum (n = 8). **(C)** Levels of GSH in serum (n = 8). **(D)** The ratio of GSH to GSSG (n = 8). **(E)** Levels of TNF-α in serum (n = 8). **(F)** Levels of IL-1β in serum (n = 8). **(G)** Levels of IL-6 in serum (n = 8). Quantitative data are shown as the mean ± SD, *$P < 0.05$, **$P < 0.01$, ***$P < 0.001$, ****$P < 0.0001$.

secondary antibody at room temperature for 1 h. After another PBS wash, DAB staining was performed for 20 min. Finally, the sections were counterstained with hematoxylin and observed after mounting.

2.21. Western blotting assay

Protein lysis buffer was added to RAW264.7 cells or mice lung and kidney tissues, followed by on-ice lysis for 30 min. After centrifugation at 16,000 rpm for 20 min at 4 °C, the supernatant was collected and mixed with protein loading buffer, boiled, and then stored in −80 °C. Prepared protein samples were subjected to SDS-PAGE gel electrophoresis and subsequently transferred onto a PVDF membrane. After blocking with 5 % skimmed milk for 1 h, the membrane was incubated overnight with the corresponding primary antibody. Following washes the next day, the membrane was incubated with an HRP-conjugated secondary antibody at room temperature for 1 h. Finally, the ECL substrate was applied for visualization, followed by photography and analysis.
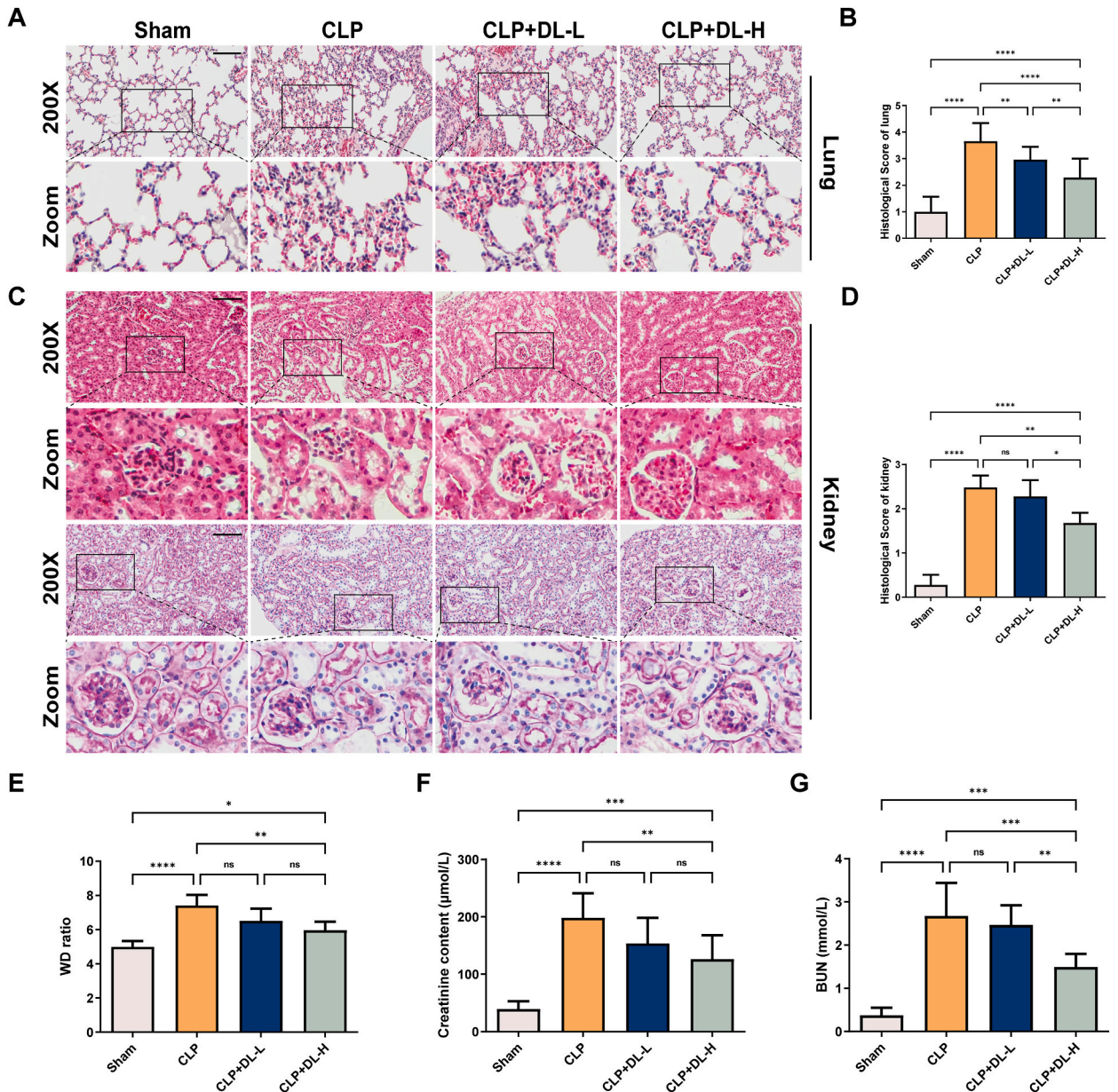

Fig. 2. Danlou tablet alleviates lung and kidney injuries in CLP mice. **(A)** HE staining images of mouse lung. Scale bar = 50 μm. **(B)** Lung injury score. **(C)** The HE and PAS staining images of mouse kidney. Scale bar = 50 μm. **(D)** Kidney injury score. **(E)** Wet-to-dry weight ratio of mouse lung (n = 8). **(F)** Levels of creatinine in serum (n = 8). **(G)** Levels of blood urea nitrogen in serum (n = 8). Quantitative data are shown as the mean ± SD, *$P < 0.05$, **$P < 0.01$, ***$P < 0.001$, ****$P < 0.0001$.

2.22. Statistical analysis

Data are expressed as mean ± SD. Statistical analysis was conducted using GraphPad Prism 9 software. One-way analysis of variance (ANOVA) was employed for inter-group comparisons, followed by Tukey's test to identify specific differences. Statistical significance was set at $P < 0.05$.

3. Results

3.1. DLT attenuates sepsis-induced inflammatory response and oxidative stress

Fig. 1A illustrates the comprehensive experimental timeline conducted in vivo. GSSG levels were increased, and GSH levels and GSH/GSSG ratio were decreased in CLP group compared with the sham group. While treatment with DLT reversed these changes, with a more pronounced reversal observed in the DL-H group (Fig. 1B–D). ELISA results indicated a significant elevation in inflammatory cytokines TNF-α, IL-1β, and IL-6 levels in CLP mice. The mice treated with DLT exhibited a reduction in the levels of these inflammatory cytokines, particularly in the DL-H group (Fig. 1E–G). These findings suggest that DLT effectively suppresses systemic oxidative stress and inflammatory response in CLP mice.

3.2. DLT alleviates lung and kidney injuries in CLP mice

The HE and PAS staining revealed marked damage in the lung and kidney tissues of CLP mice compared to the sham group, with higher injury scores (Fig. 2A–D). Following DLT treatment, these changes were alleviated, particularly in the DL-H group (Fig. 2A–D). Additionally, the lung wet-to-dry weight ratio significantly increased in CLP mice, while it decreased in the DL-H group (Fig. 2E). Biochemical analysis of blood parameters indicated a significant elevation in serum creatinine and BUN levels in CLP mice compared to the sham group, which were reduced in the DL-H group (Fig. 2F and G). These results suggest that DLT mitigates structural and functional damage in the lung and kidney tissues of CLP mice.

3.3. Identification and enrichment analysis of regulatory targets of DLT in treating sepsis

We retrieved active components of DLT and their corresponding regulatory targets from the TCMSP database. Additionally, 3725 targets associated with sepsis were obtained. The intersection of drug regulatory targets and sepsis-related targets yielded 55 potential
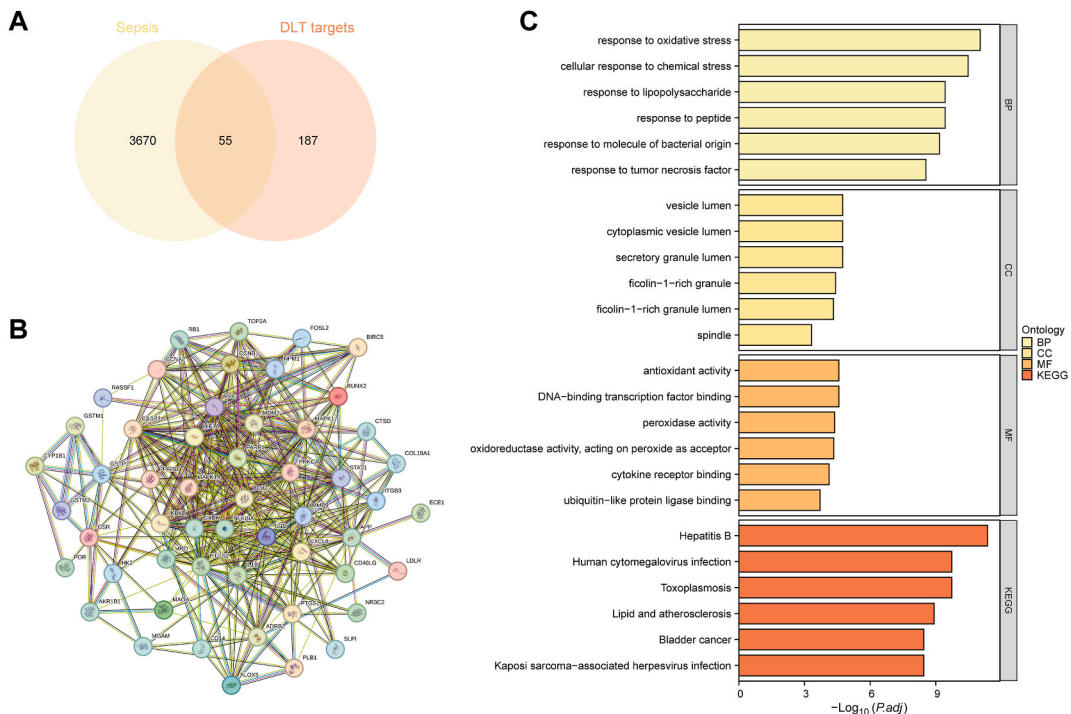

Fig. 3. Identification and enrichment analysis of regulatory targets of Danlou tablet in treating sepsis. **(A)** Venn diagram demonstrating potential targets for DLT in the treatment of sepsis. **(B)** Protein-protein interaction network for potential targets. **(C)** Enrichment analyses of potential targets using Gene Ontology (GO) and Kyoto Encyclopedia of Genes and Genomes analyses (KEGG).

targets for DLT therapy in sepsis (Fig. 3A). A protein-protein interaction network was constructed for these 55 potential targets, followed by functional and pathway enrichment analyses (Fig. 3B and C). The results of the enrichment analysis indicated that the top 3 enriched GO biological processes (BPs) among these targets were response to oxidative stress, response to chemical stress, and response to lipopolysaccharide. The top three enriched GO cellular components (CCs) were the vesicle lumen, cytoplasmic vesicle lumen, and secretory granule lumen. The leading three molecular functions (MFs) included antioxidant activity, DNA-binding transcription factor binding, and peroxidase activity. These 55 potential targets associated with the organ-protective effects of DLT in treating sepsis were predominantly distributed in pathways related to Hepatitis B, human cytomegalovirus infection, and toxoplasmosis.
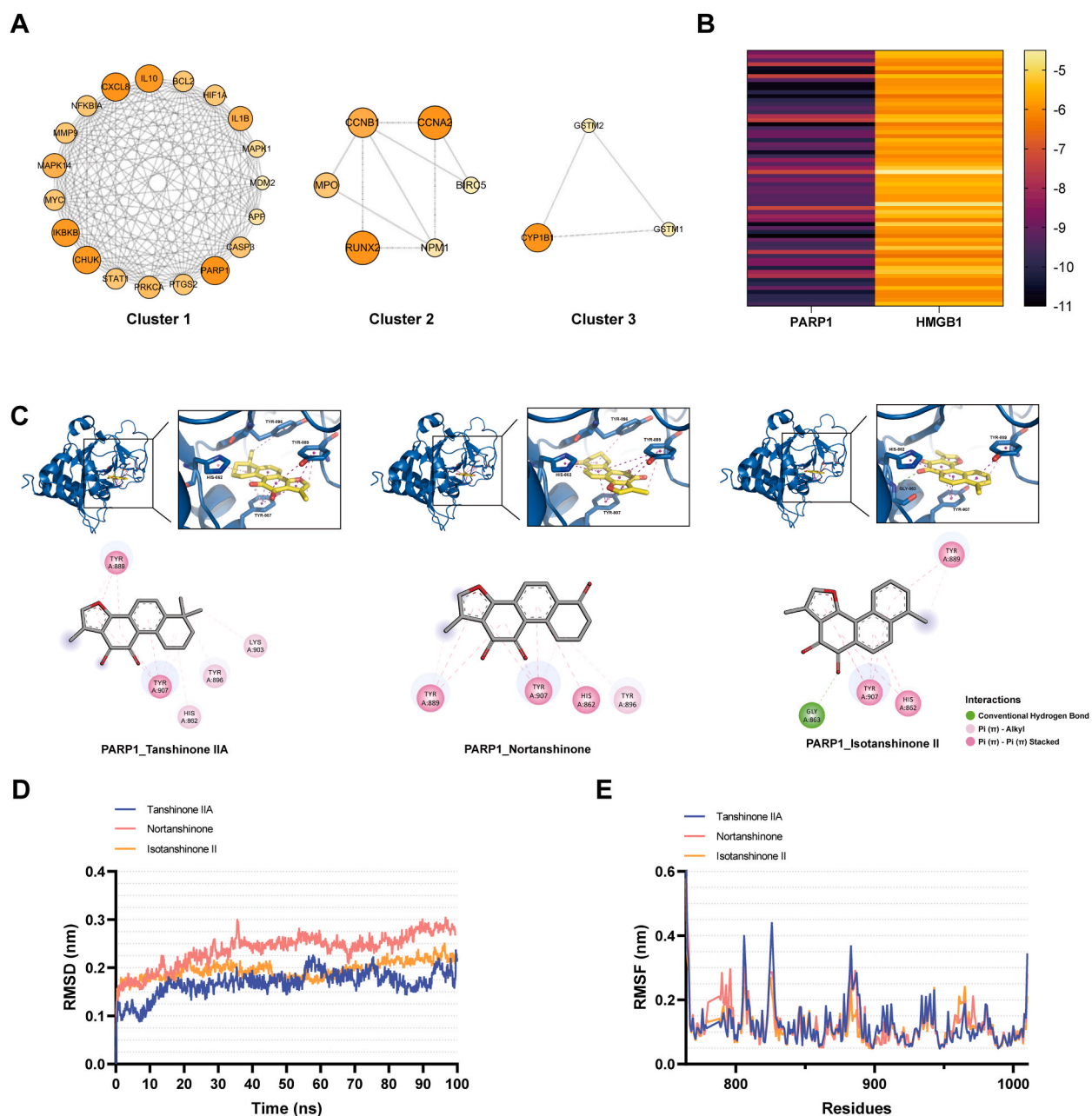
Fig. 4. Candidate target selection and molecular docking. **(A)** Key therapeutic targets. **(B)** The heatmap of binding affinity of PARP1 and HMGB1 combined with active compounds in DLT. **(C)** The representative docking complex of key targets and compounds. **(D)** RMSD values of PARP1 and the key compounds. **(E)** RMSF values of PARP1 and the key compounds.
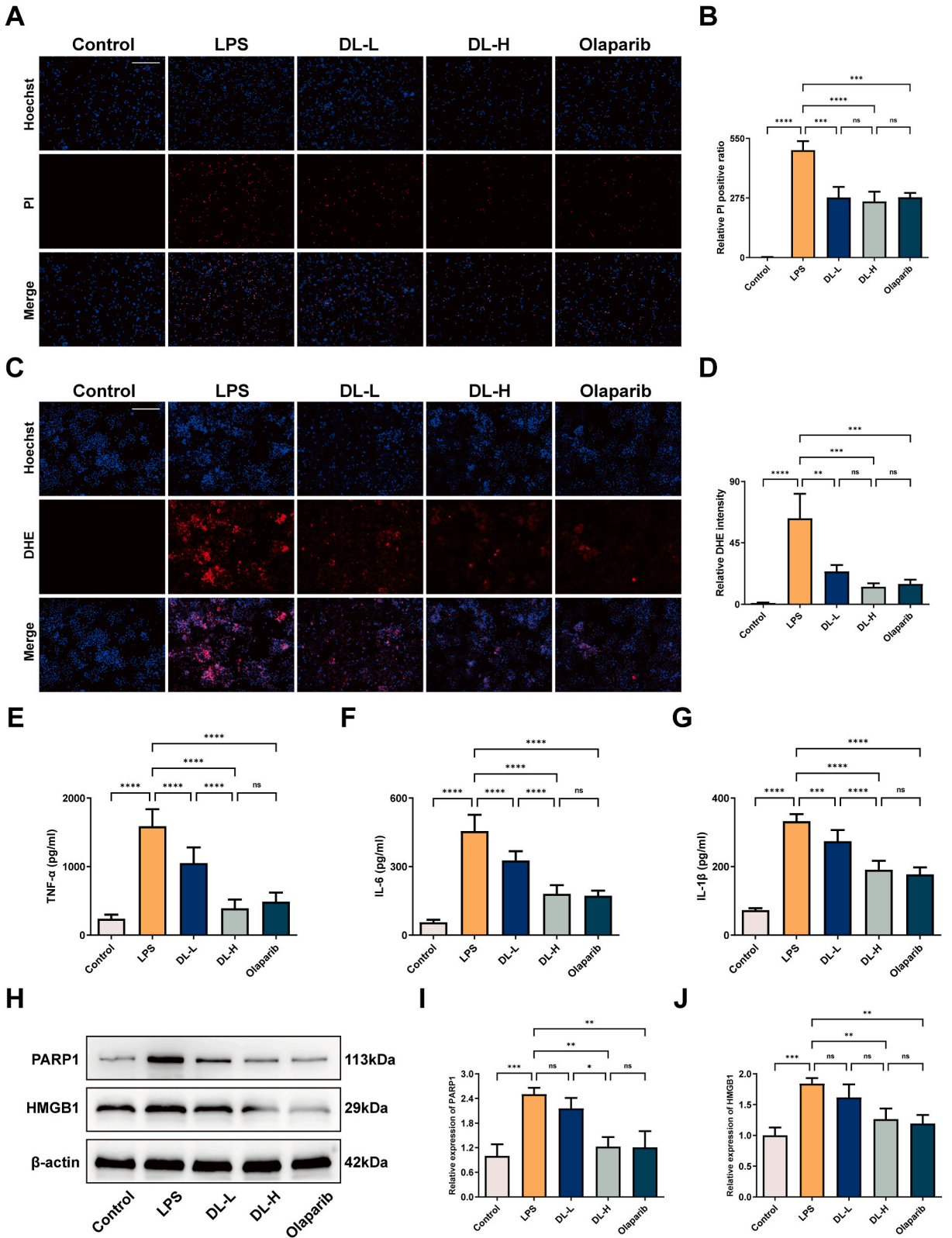
(caption on next page)

Fig. 5. Protective effects of Danlou tablet on LPS-treated macrophages. **(A)** PI staining images of RAW264.7 cells. Scale bar = 200 μm. **(B)** PI-positive cell rate (n = 3). **(C)** DHE staining images of RAW264.7 cells. Scale bar = 200 μm. **(D)** Statistical analysis of relative fluorescence intensity in DHE staining (n = 3). **(E)** Levels of TNF-α in RAW264.7 cells (n = 8). **(F)** Levels of IL-6 in RAW264.7 cells (n = 8). **(G)** Levels of IL-1β in RAW264.7 cells (n = 8). **(H–J)** The protein levels of PARP1 and HMGB1 in RAW264.7 cells (n = 3). Quantitative data are shown as the mean ± SD, *$P < 0.05$, **$P < 0.01$, ***$P < 0.001$, ****$P < 0.0001$.

3.4. Candidate target selection and molecular docking

To identify key targets of DLT in treating sepsis, the MCODE algorithm was employed to screen the key targets in the protein-protein interaction network. Notably, PARP1 exhibited a high score within cluster 1, prompting its selection for further analysis
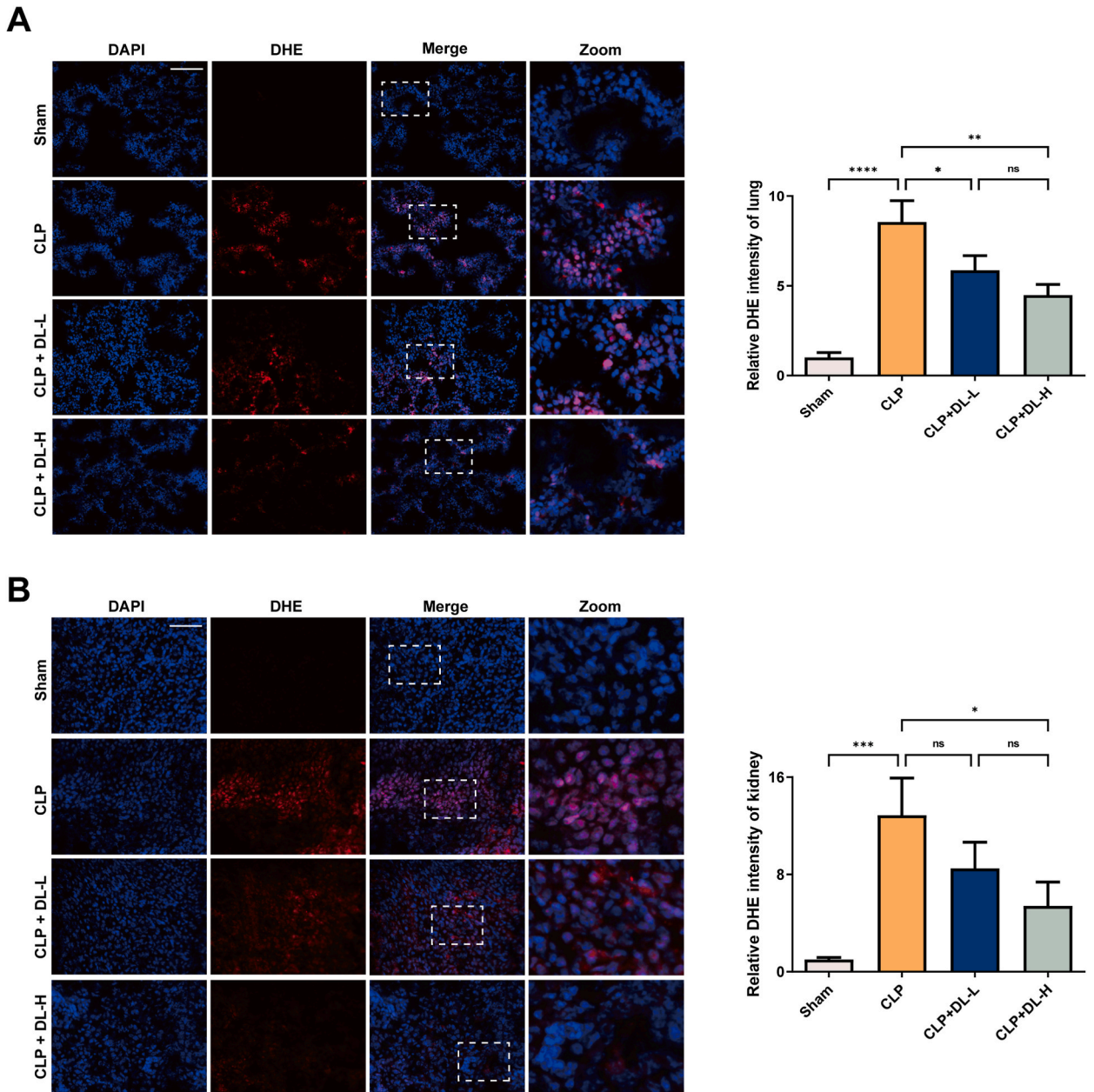
Fig. 6. Danlou tablet alleviates oxidative stress in lung and kidney tissues of CLP mice. **(A)** DHE staining and fluorescence intensity analysis of lungs (n = 3). Scale bar = 50 μm. **(B)** DHE staining and fluorescence intensity analysis of kidneys (n = 3). Scale bar = 50 μm. Quantitative data are shown as the mean ± SD, *$P < 0.05$, **$P < 0.01$, ***$P < 0.001$, ****$P < 0.0001$.

(Fig. 4A). To identify potential active compounds in DLT capable of modulating PARP1 and its downstream target HMGB1, we conducted molecular docking of all DLT active compounds with PARP1 and HMGB1 proteins, revealing a generally higher binding affinity of DLT compounds to PARP1 compared to HMGB1 (Fig. 4B and C). This suggests that active compounds in DLT may exert a more pronounced regulatory effect on PARP1. Ultimately, the top three active compounds in DLT with higher binding affinity to PARP1 (Tanshinone IIA, Nortanshinone, and Isotanshinone II) were subjected to molecular dynamics simulations with PARP1 protein. The results demonstrate that all three compounds mentioned can stably bind to the PARP1 protein (Fig. 4D and E).

3.5. Protective effects of DLT on LPS-treated macrophages

To investigate the regulatory effects of DLT on macrophages under septic conditions and elucidate its mechanism, we stimulated RAW264.7 cells with LPS and treated them with serum containing DLT or the PARP1 inhibitor Olaparib. PI staining revealed a significant increase in cell death rate in the LPS group compared to the Control group. However, cells treated with serum containing DLT or Olaparib exhibited a reduced cell death rate compared to the LPS group (Fig. 5A and B). DHE staining showed a significant elevation in superoxide anion levels in LPS-stimulated cells, which was mitigated in cells treated with serum containing DLT or Olaparib (Fig. 5C and D). Levels of inflammatory cytokines TNF-α, IL-6, and IL-1β significantly increased in LPS-stimulated cells, and these changes were alleviated in cells treated with serum containing DLT or Olaparib (Fig. 5E–G). Additionally, the expression levels of PARP1 and HMGB1 proteins, elevated in LPS-treated cells, were downregulated in cells treated with serum containing DLT or Olaparib (Fig. 5H–J). These findings suggest that DLT alleviates macrophage death, oxidative stress, and pro-inflammatory responses induced by LPS, and its mechanism involves the inhibition of PARP1 and HMGB1.
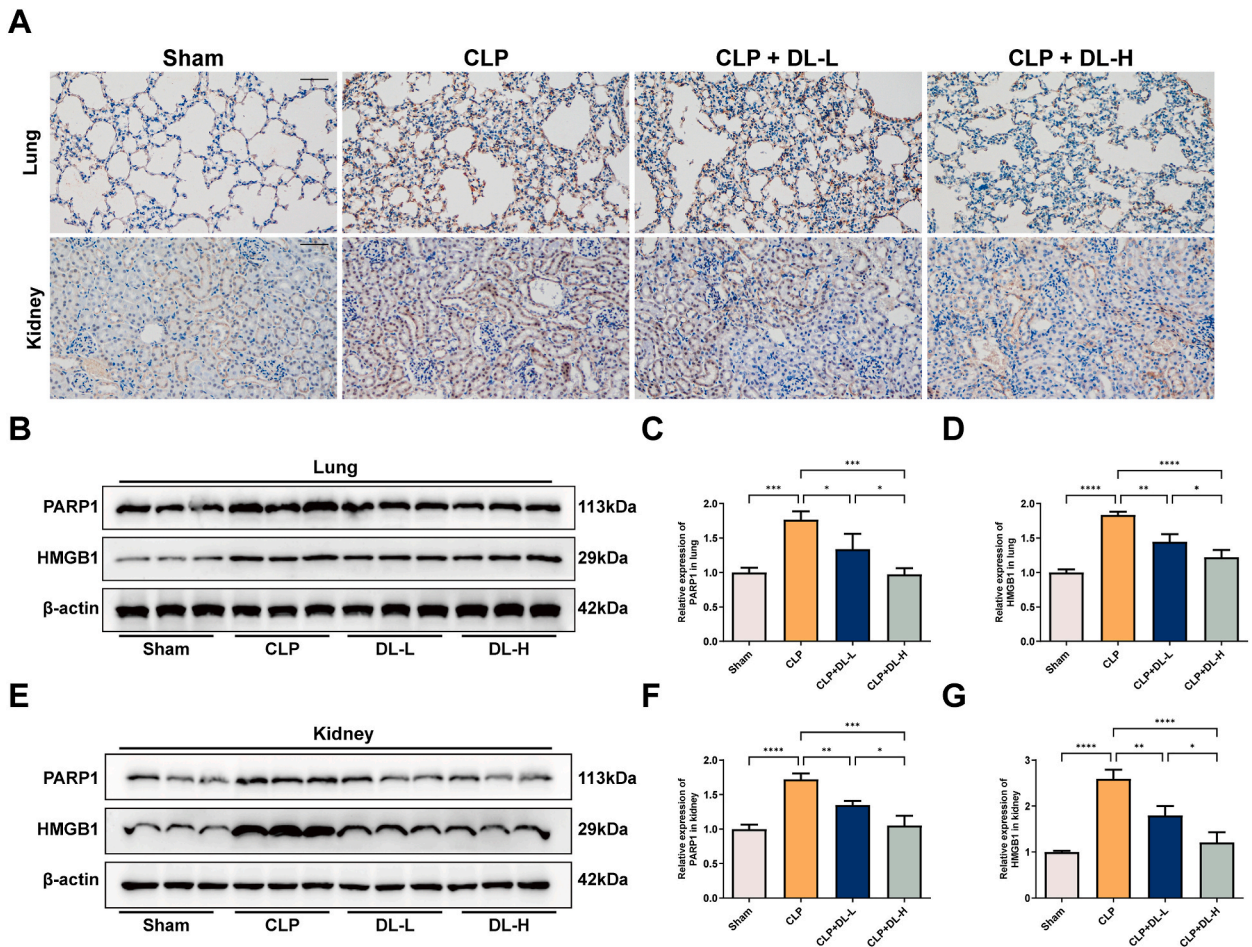

Fig. 7. Danlou tablet inhibits the PARP1/HMGB1 signaling pathway in CLP mice. **(A)** Immunohistochemical staining of PARP1 in mice lung and kidney tissues. Scale bar = 50 μm. **(B–D)** The protein levels of PARP1 and HMGB1 in mice lungs (n = 3). **(E–G)** The protein levels of PARP1 and HMGB1 in mice kidneys (n = 3). Quantitative data are shown as the mean ± SD, $*P < 0.05$, $**P < 0.01$, $***P < 0.001$, $****P < 0.0001$.

3.6. DLT inhibits the PARP1/HMGB1 signaling pathway in CLP mice

As shown in Fig. 6A and B, compared to the sham group, mice in the CLP group exhibited a significant increase in superoxide anion levels in lungs and kidneys. However, in the DL-L and DL-H groups, the levels of superoxide anions in lungs and kidneys were reduced compared to the CLP group, with a more pronounced reduction in the DL-H group. Immunohistochemical staining revealed a significant upregulation of PARP1 in lungs and kidneys of CLP mice, whereas mice treated with DLT showed significant downregulation of PARP1 (Fig. 7A). Western blot results similarly demonstrated downregulation of PARP1 and HMGB1 in lungs and kidneys of DL-L and DL-H groups compared to CLP group (Fig. 7B–G). These results suggest that DLT treatment significantly reduces oxidative stress in tissues of CLP mice, and its mechanism may be associated with the inhibition of the PARP1/HMGB1 signaling pathway.

4. Discussion

TCM has a long history and has been used extensively, emphasizing individualized treatment and a holistic approach, which provide unique advantages in the treatment of sepsis [11]. In recent years, there has been increasing research interest in applying TCM in sepsis treatment to explore its therapeutic efficacy and mechanisms. Therefore, discovering novel TCM interventions for sepsis and elucidating their mechanisms holds significant promise in improving sepsis prognosis [21]. DLT, a TCM formulation, possesses pharmacological effects such as fever reduction, detoxification, and promotion of blood circulation and has been widely used to treat various diseases. The study confirms the therapeutic efficacy of DLT in anti-inflammatory and antioxidant activities [12–14]. Delving into the therapeutic potential of DLT for sepsis and analyzing its underlying mechanisms holds positive implications for organ function protection in sepsis.

The experiment showed that DLT significantly alleviated systemic oxidative stress and inflammation levels in CLP mice. Moreover, DLT also attenuated the pro-inflammatory response of LPS-treated macrophages, reducing the rate of macrophage death and oxidative stress. This indicates the promising therapeutic efficacy of DLT in sepsis. Further investigations revealed that DLT effectively mitigates structural and functional abnormalities in the lung and kidney tissues of CLP mice. To explore the regulatory mechanisms of DLT, we identified 55 intersecting targets between sepsis-related targets and DLT-related targets. Protein-protein interaction analysis led to the identification of the key molecule Poly(ADP-Ribose) Polymerase 1 (PARP1). PARP1 is a highly conserved protein, and previous literature has reported that PARP1 is a cleavage substrate for cysteine asparaginase, which plays an important role in apoptosis [22]. In certain pathological conditions, hyperactivation of PARP1 can lead to increased cellular damage and ultimately death [23]. Research indicates that PARP1 increases the inflammatory response to bacterial infection-induced sepsis by regulating the transcription and activation of inflammatory factors in myeloid cells [24]. Inhibiting PARP1 effectively alleviates lung injury severity in LPS-induced acute lung injury mice [25]. Additionally, in LPS-stimulated macrophages, PARP1 promotes the release of high mobility group protein (HMGB1) [26]. HMGB1 is an evolutionarily highly conserved protein that can be released by activated macrophages, mediating inflammatory responses [27–29]. Clinical studies have shown a significant elevation in circulating HMGB1 levels in septic patients, positively correlating with the severity of sepsis and mortality [30,31]. Therefore, inhibiting the PARP1/HMGB1 signaling pathway in macrophages improves organ dysfunction caused by sepsis [26]. In this experiment, we observed an upregulation of PARP1 and HMGB1 protein expression in the lung and kidney tissues of CLP mice. Additionally, macrophages stimulated with LPS showed increased expression of PARP1 and HMGB1 proteins. Treatment with DLT in mice or macrophages reversed these changes, indicating the significant role of the PARP1/HMGB1 signaling pathway in the DLT-mediated improvement of organ dysfunction induced by sepsis. However, the specific active components responsible for this process still need to be clarified.

To identify the primary constituents in DLT regulating PARP1/HMGB1 signaling pathway, we conducted bulk molecular docking between active components in DLT and these two proteins. The results indicate a higher binding affinity between DLT's active components and PARP1, while the binding affinity with HMGB1 is lower. This suggests that DLT's regulatory effect on the PARP1/HMGB1 signaling pathway may primarily involve the modulation of the PARP1 protein. The top three compounds with the highest binding affinity to PARP1 are Tanshinone IIA, Isotanshinone II, and Nortanshinone. Studies have shown that Tanshinone IIA can effectively alleviate sepsis-induced immunosuppression, enhancing survival in the CLP mouse model [32]. Tanshinone IIA can alleviate sepsis-induced acute lung injury by regulating the ROCK2/NF-κB signaling axis [33]. Tanshinone IIA also ameliorated sepsis-induced renal tissue injury and renal cell apoptosis, reduced serum levels of creatinine and urea nitrogen, and down-regulated TNF-α, IL-6, and IL-1β expression [34]. Furthermore, Tanshinone IIA has been demonstrated to exert protective effects on the intestines, cardiovascular system, and coagulation function under septic conditions [35–37]. The above studies provide a partial theoretical basis for DLT in the treatment of sepsis. However, there are currently no reported associations between Tanshinone IIA and the regulation of PARP1 protein. Our molecular docking results suggest a strong binding affinity between Tanshinone IIA and PARP1, indicating its potential regulatory effect on PARP1, warranting further exploration. Limited research is available on Isotanshinone II and Nortanshinone. Although our molecular docking results suggest their potential regulatory effect on PARP1 protein, their specific pharmacological actions require further observation. While our research findings demonstrate the regulatory potential of the compounds above on PARP1, the mechanism underlying their ability to downregulate PARP1 protein levels remains elusive. The mechanism may involve these compounds' regulation of post-translational modifications of PARP1, such as ubiquitination, thereby influencing the protein expression levels of PARP1. The specific details of the regulatory mechanism require further elucidation.

For the first time, this study investigates the therapeutic effects of DLT on organ dysfunction induced by sepsis and its regulatory impact on macrophages and explores the underlying mechanism. However, the study has the following limitations. First, we only focused on the regulatory effects of DLT on sepsis-induced ALI and AKI, while its impact on other organs remains unknown. Second, this study focused on the pro-inflammatory response of macrophages and CLP mice, but did not detect the expression of anti-

inflammatory cytokines, which needs to be further explored in future experiments. Third, the therapeutic mechanism of DLT was selectively validated and discussed through protein-protein interaction analysis, neglecting the exploration of other potential mechanisms. Fourth, no individual functional validation was conducted for the key active compounds in DLT. Future research efforts will address these limitations and strive for improvement.

5. Conclusions

This study demonstrates that DLT inhibits macrophage pro-inflammatory responses, alleviates excessive inflammation and oxidative stress in septic mice, and improves lung and kidney injury. Additionally, through bioinformatics analysis, molecular docking techniques, and in vivo and in vitro experiments, it was found that DLT's anti-inflammatory and antioxidant effects are associated with the regulation of the PARP1/HMGB1 signaling pathway. The research confirms the therapeutic effects of DLT on sepsis and its associated organ dysfunction, elucidates the treatment mechanisms, and identifies potential key compounds in this process, providing a scientific foundation for DLT in sepsis treatment.

Ethics statement

The animal study protocol was approved by the Ethics Committee of the Second Affiliated Hospital of Harbin Medical University (Approval No. SYDW 2021–087).

Data availability statement

Data will be made available on request.

CRediT authorship contribution statement

Yongjing Yu: Writing – original draft, Supervision, Methodology, Conceptualization. **Zhixi Li:** Visualization, Software, Methodology. **Chang Liu:** Visualization, Methodology, Data curation. **Yue Bu:** Methodology. **Weidong Gong:** Methodology. **Juan Luo:** Methodology. **Ziyong Yue:** Writing – review & editing, Supervision, Conceptualization.

Declaration of competing interest

The authors declare that they have no known competing financial interests or personal relationships that could have appeared to influence the work reported in this paper.

Appendix A. Supplementary data

Supplementary data to this article can be found online at https://doi.org/10.1016/j.heliyon.2024.e30172.

References

[1] M. Singer, et al., The third international consensus definitions for sepsis and septic shock (Sepsis-3), JAMA 315 (8) (2016) 801–810, https://doi.org/10.1001/jama.2016.0287.

[2] B. Gibson, C. Terblanche, Anaesthetic management of patients with severe sepsis, Br. J. Anaesth. 106 (3) (2011) 416–417, https://doi.org/10.1093/bja/aer015, author reply 417.

[3] K.E. Rudd, et al., Global, regional, and national sepsis incidence and mortality, 1990-2017: analysis for the Global Burden of Disease Study, Lancet 395 (10219) (2020) 200–211, https://doi.org/10.1016/s0140-6736(19)32989-7.

[4] S. Rungsung, et al., Luteolin attenuates acute lung injury in experimental mouse model of sepsis, Cytokine 110 (2018) 333–343, https://doi.org/10.1016/j.cyto.2018.03.042.

[5] S. Peerapornratana, et al., Acute kidney injury from sepsis: current concepts, epidemiology, pathophysiology, prevention and treatment, Kidney Int. 96 (5) (2019) 1083–1099, https://doi.org/10.1016/j.kint.2019.05.026.

[6] C.L. Klein, et al., Interleukin-6 mediates lung injury following ischemic acute kidney injury or bilateral nephrectomy, Kidney Int. 74 (7) (2008) 901–909, https://doi.org/10.1038/ki.2008.314.

[7] H. Rabb, et al., Acute renal failure leads to dysregulation of lung salt and water channels, Kidney Int. 63 (2) (2003) 600–606, https://doi.org/10.1046/j.1523-1755.2003.00753.x.

[8] T.S. Hoke, et al., Acute renal failure after bilateral nephrectomy is associated with cytokine-mediated pulmonary injury, J. Am. Soc. Nephrol. 18 (1) (2007) 155–164, https://doi.org/10.1681/asn.2006050494.

[9] F. Chen, et al., Targeting toll-like receptors in sepsis: from bench to clinical trials, Antioxidants Redox Signal. 35 (15) (2021) 1324–1339, https://doi.org/10.1089/ars.2021.0005.

[10] Z.B. Lu, et al., Heat-clearing Chinese medicines in lipopolysaccharide-induced inflammation, Chin. J. Integr. Med. 26 (7) (2020) 552–559, https://doi.org/10.1007/s11655-020-3256-7.

[11] Y. Song, W. Lin, W. Zhu, Traditional Chinese medicine for treatment of sepsis and related multi-organ injury, Front. Pharmacol. 14 (2023) 1003658, https://doi.org/10.3389/fphar.2023.1003658.

[12] D. Hao, et al., Ethanol extracts of Danlou tablet attenuate atherosclerosis via inhibiting inflammation and promoting lipid effluent, Pharmacol. Res. 146 (2019) 104306, https://doi.org/10.1016/j.phrs.2019.104306.

[13] S. Gao, et al., Danlou tablet inhibits the inflammatory reaction of high-fat diet-induced atherosclerosis in ApoE knockout mice with myocardial ischemia via the NF-κB signaling pathway, J. Ethnopharmacol. 263 (2020) 113158, https://doi.org/10.1016/j.jep.2020.113158.

[14] C. Liu, et al., Danlou tablet attenuates ischemic stroke injury and blood–brain barrier damage by inhibiting ferroptosis, J. Ethnopharmacol. 322 (2023) 117657, https://doi.org/10.1016/j.jep.2023.117657.

[15] R. Chen, et al., Danlou tablet inhibits high-glucose-induced cardiomyocyte apoptosis via the miR-34a-SIRT1 axis, Heliyon 9 (3) (2023) e14479, https://doi.org/10.1016/j.heliyon.2023.e14479.

[16] D. Rittirsch, et al., Immunodesign of experimental sepsis by cecal ligation and puncture, Nat. Protoc. 4 (1) (2009) 31–36, https://doi.org/10.1038/nprot.2008.214.

[17] L. Wang, et al., Danlou tablet activates autophagy of vascular adventitial fibroblasts through PI3K/Akt/mTOR to protect cells from damage caused by atherosclerosis, Front. Pharmacol. 12 (2021) 730525, https://doi.org/10.3389/fphar.2021.730525.

[18] S. Ma, et al., Qian Yang Yu Yin granule improves hypertensive renal damage: a potential role for TRPC6-CaMKKβ-AMPK-mTOR-mediated autophagy, J. Ethnopharmacol. 302 (Pt A) (2023) 115878, https://doi.org/10.1016/j.jep.2022.115878.

[19] G. Matute-Bello, et al., An official American Thoracic Society workshop report: features and measurements of experimental acute lung injury in animals, Am. J. Respir. Cell Mol. Biol. 44 (5) (2011) 725–738, https://doi.org/10.1165/rcmb.2009-0210ST.

[20] Y. Zhou, W. Xu, H. Zhu, CXCL8((3-72)) K11R/G31P protects against sepsis-induced acute kidney injury via NF-κB and JAK2/STAT3 pathway, Biol. Res. 52 (1) (2019) 29, https://doi.org/10.1186/s40659-019-0236-5.

[21] T.T. Fan, et al., Application of Chinese medicine in the management of critical conditions: a review on sepsis, Am. J. Chin. Med. 48 (6) (2020) 1315–1330, https://doi.org/10.1142/s0192415x20500640.

[22] R.J. Henning, M. Bourgeois, R.D. Harbison, Poly(ADP-ribose) Polymerase (PARP) and PARP inhibitors: mechanisms of action and role in cardiovascular disorders, Cardiovasc. Toxicol. 18 (6) (2018) 493–506, https://doi.org/10.1007/s12012-018-9462-2.

[23] M. Scheffner, U. Nuber, J.M. Huibregtse, Protein ubiquitination involving an E1-E2-E3 enzyme ubiquitin thioester cascade, Nature 373 (6509) (1995) 81–83, https://doi.org/10.1038/373081a0.

[24] F.A. Kunze, et al., ARTD1 in myeloid cells controls the IL-12/18-IFN-γ Axis in a model of sterile sepsis, chronic bacterial infection, and cancer, J. Immunol. 202 (5) (2019) 1406–1416, https://doi.org/10.4049/jimmunol.1801107.

[25] G. Wang, et al., PARP-1 inhibitor, DPQ, attenuates LPS-induced acute lung injury through inhibiting NF-κB-mediated inflammatory response, PLoS One 8 (11) (2013) e79757, https://doi.org/10.1371/journal.pone.0079757.

[26] Z. Yang, et al., PARP-1 mediates LPS-induced HMGB1 release by macrophages through regulation of HMGB1 acetylation, J. Immunol. 193 (12) (2014) 6114–6123, https://doi.org/10.4049/jimmunol.1400359.

[27] H. Yang, H. Wang, U. Andersson, Targeting inflammation driven by HMGB1, Front. Immunol. 11 (2020) 484, https://doi.org/10.3389/fimmu.2020.00484.

[28] M. Deng, et al., The endotoxin delivery protein HMGB1 mediates caspase-11-dependent lethality in sepsis, Immunity 49 (4) (2018) 740–753.e7, https://doi.org/10.1016/j.immuni.2018.08.016.

[29] U. Andersson, K.J. Tracey, HMGB1 is a therapeutic target for sterile inflammation and infection, Annu. Rev. Immunol. 29 (2011) 139–162, https://doi.org/10.1146/annurev-immunol-030409-101323.

[30] J. Sundén-Cullberg, et al., Persistent elevation of high mobility group box-1 protein (HMGB1) in patients with severe sepsis and septic shock, Crit. Care Med. 33 (3) (2005) 564–573, https://doi.org/10.1097/01.ccm.0000155991.88802.4d.

[31] S. Karlsson, et al., HMGB1 as a predictor of organ dysfunction and outcome in patients with severe sepsis, Intensive Care Med. 34 (6) (2008) 1046–1053, https://doi.org/10.1007/s00134-008-1032-9.

[32] M. Gao, et al., Tanshinone IIA attenuates sepsis-induced immunosuppression and improves survival rate in a mice peritonitis model, Biomed. Pharmacother. 112 (2019) 108609, https://doi.org/10.1016/j.biopha.2019.108609.

[33] J. Liu, et al., Tanshinone IIA improves sepsis-induced acute lung injury through the ROCK2/NF-κB axis, Toxicol. Appl. Pharmacol. 446 (2022) 116021, https://doi.org/10.1016/j.taap.2022.116021.

[34] Z.Y. Chen, et al., Tanshinone IIA alleviates acute liver and kidney injury in septic rats, Chinese Journal of Immunology 36 (13) (2020) 1578–1582.

[35] W. Zhu, et al., Protective effect of sodium tanshinone IIA sulfonate on injury of small intestine in rats with sepsis and its mechanism, Chin. J. Integr. Med. 18 (7) (2012) 496–501, https://doi.org/10.1007/s11655-011-0942-5.

[36] Z.J. Meng, et al., Sodium tanshinone IIA sulfonate attenuates cardiac dysfunction and improves survival of rats with cecal ligation and puncture-induced sepsis, Chin. J. Nat. Med. 16 (11) (2018) 846–855, https://doi.org/10.1016/s1875-5364(18)30126-2.

[37] W. Zhu, et al., Sodium tanshinone II A sulfonate ameliorates microcirculatory disturbance of small intestine by attenuating the production of reactie oxygen species in rats with sepsis, Chin. J. Integr. Med. 22 (10) (2016) 745–751, https://doi.org/10.1007/s11655-015-2083-8.